Intermetallic Compounds In The Al-Si-Cu System

C. Triveño Rios[1]; R. Caram[2]; C. Bolfarini[1]; W.J. Botta F.[1] and C.S. Kiminami[1]
[1]*Federal University of São Carlos, Department of Materials Engineering*
[2]*State University of Campinas, Department of Materials Engineering*
P. O Box 676, 13565-190 São Carlos, SP, Brasil

Abstract

An understanding of the nature and the formation of the intermetallic compounds in alloys of the Al-Si-Cu system is of importance, especially when its origin is of secondary sources, as recycled aluminum. The main objective of this study was to analyze the morphology and composition of complex microstructures of the intermetallic phases in the Al-Si-Cu alloys. The as-cast microstructures consisted of several phases; α-Al, Si, Al_2Cu, λ-$Al_5Mg_9Si_6Cu_2$, β-Al_5FeSi π-$Al_8Si_6Mg_3Fe$, e α-$Al_{15}(Mn,Fe)_3Si_2$ and of other phases in formation. The most common morphology was the Chinese-script, however, in high iron concentrations the dominant morphology was of the platelets of β-Al_5FeSi phase. Also, it was observed that those phases are highly brittle.

Keywords: Al-Si-Cu System, Intermetallic Compounds, Aluminum Alloys, Iron.

Introduction

Aluminum and aluminum alloys represent an important category of materials due to their high technological value and wide range of applications, especially in aerospace, automotive and household industries. The alloys of the Al-Si-Cu system have become increasingly important in recent years, mainly in the automotive industry that uses secondary aluminum (recycled) in the form of various motor mounts, pistons, cylinder heads, heat exchangers, air conditioners, transmission housings, wheels, fenders, loads floors and suspension components due to their high strength at room and high temperature [1]. However, these aluminum-base systems usually contain a certain amount of Fe, Mn and Mg that are present either undeliberately, or they are added deliberately to provide special material properties. The presence of some magnesium improves the hardenability of the material and some manganese is usually added to reduce the detrimental effects of impurities like iron and silicon. Depending on the purity of the base material, the impurities and alloying elements partially go into α-Al solid solution and partly form intermetallic particles. During the solidification process enormous variety of intermetallic compounds are formed, at the grain boundaries and between the dendritic arms. Among all the elements, iron is probably the most important one, because it forms brittle and hard intermetallic compounds like α-$Al_{15}(Mn,Fe)_3Si_2$ and β-Al_5FeSi. They are hard to dissolve during homogenization and are detrimental to the mechanical properties of the alloys [2]. Also, they may act as stress raiser, since they present low ductility and fracture toughness at ambient temperature. In contrast, they present inadequate strength and creep resistance at elevated temperatures. The objective of the present study is to analyze the morphology and composition of complex microstructures containing intermetallic phases formed in the Al-Si-Cu alloys.

Materials and Methods

In the present work, preliminary were analyzed three alloys, with nominal compositions given in the table 1. The alloys were prepared using metallic elements of commercial purity. First, the elements of the alloys 1 and 2 were melted in an electrical resistance furnace and after, the melting was performed in an arc furnace with water-cooled cooper hearth under inert atmosphere, in order to ensure the homogeneity and increase the cooling rate. Deliberately were added Fe particles in the Al-5.5Si-3.5Cu-0.3Mg alloy with the purpose to promote the formation of intermetallic compounds. The alloy 3 was melted at 750°C in graphite crucible in an electrical resistance furnace and cooled in an iron mold previously heated without control of temperature. The samples were prepared by standard metallographic procedures (mechanically polished in slurry of diamond and alumina and etched with solution of 5 grams of NaOH in H_2O).

The microstructure was analyzed using optical microscopy. To determine the characteristics and composition of the solidified phases, scanning electronic microscopy (SEM) equipped with energy dispersive spectroscopy (EDS) was employed.

Table 1: Nominal composition of the studied alloys

Alloy	wt%				
	Si	Cu	Fe	Mg	Mn
1	5.5	3.5	*	0.3	--
2	8,5	2.5	0,4	0.3	0.1
3	10.1	4.6	1.2	0.1	0.15

* Added particles

Results and Discussion

Firstly the alloy 1 was analyzed. May be observed in the figure 1, that the Fe did not dissolve in the Al-5.5Si-3.5Cu-0.3Mg alloy, and it originated an Fe/Al-5.5Si-3.5Cu-0.3Mg interface. The formation of that interface is due to the low solubility of Fe in the α-Al matrix. According to Mondolfo [3], the maximum solubility in equilibrium is 0.05wt% Fe. In this interface, various intermetallic compounds consisting of ~Fe_3AlCu, ~$Al_3Fe(Mg)$ ~$Fe_7Al_4Mg_2Si_2Cu$ and Fe_3Al were found, as observed in the figure 1. The corresponding EDS spectra are shown in the figures 2a-c. These phases possibly are in the nonequilibrium state or metastable condition, indicating that diffusion between the particles and elements is not fully completed.

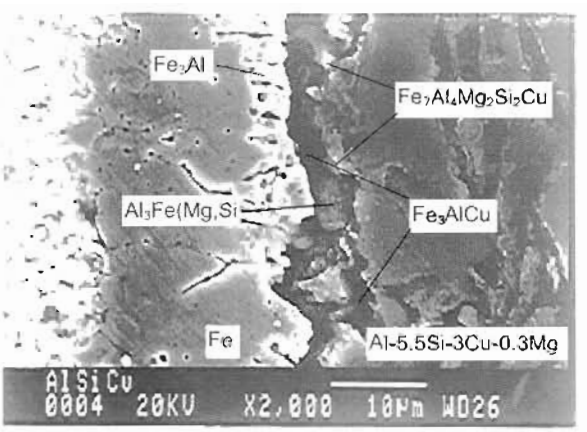

Figure 1. Fe/Al-5.5Si-3.5Cu-0.3Mg interface, showing intermetallic phases at no equilibrium state.

Figure 3 shows the typical microstructure of the alloys 2 and 3. It consisted of α-Al dendrites and interdendritic region containing Si particles and various intermetallic phases. The difference in the size of the dendrites is due to the differences in composition and to the solidification conditions. Backerud et al. [4] suggested that six reactions may occur during solidification of an alloy in the composition interval Al-(8.5-10.5)Si-(2.0-4.0)Cu-0.9Cu-0.5Mn-1.0Mg alloy, as shown in the table 2. According to this, one could expect various binary and tertiary eutectics to form in the interdendritic regions (figures 3-5).

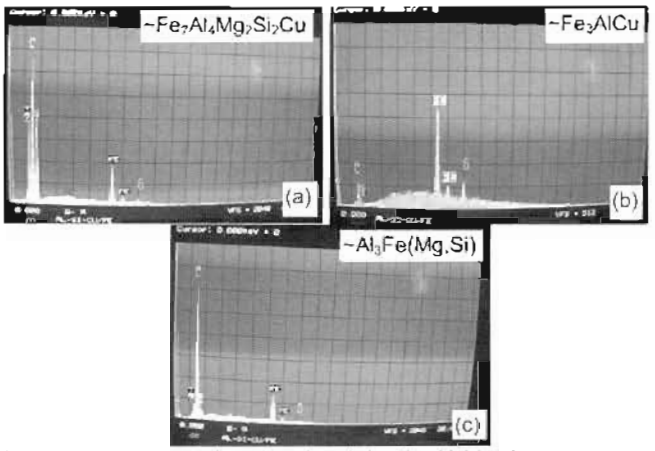

Figure 2. EDS spectra showing (a) ~$Fe_7Al_4Mg_2Si_2Cu$ phase, (b) ~Fe_3AlCu phase, (c) ~$Al_3Fe(Mg)$ phase.

Table 2. Reactions that can occurs in the Al-Si-Cu system.

N°	Reactions during the solidification [4]	Temp.°C
1	Liquid → α-Al dendrite and $Al_{15}(MnFe)_3Si_2$	~598
2	Liquid → α-Al + Si + Al_5FeSi	~575
3	Liq. → α-Al + Si + Mg_2Si + $Al_8Mg_3FeSi_6$	~554
4	Liq. + Mg_2Si + Si → α-Al + $Al_5Mg_8Si_6Cu_2$	~575
5	Liq. → α-Al + Al_2Cu + Al_5FeSi + Si	~529
6	Liq. → α-Al + Si + $Al_5Mg_8Si_6Cu_2$	~504

Observing the figures 4a-b, it is suggested that quaternary (α-Al + Si + Al_2Cu + $Al_8Mg_3FeSi_6$), ternary (Al + Si + Al_2Cu) and binary (Al + Si, Al + Al_2Cu) eutectic structures are presents in the interdendritic region. Occasionally, there were observed areas with Chinese-script morphologies of λ-$Al_5Mg_6Si_6Cu_2(Fe)$ (figure 5a), π-$Al_8Si_6Mg_3Fe(Cu)$ (figure 5b) and α-$Al_{15}(MnFe)_3Si_2$ (figure 5c) phases that usually form fine eutectic structures together with α-Al. However, the π-$Al_8Si_6Mg_3Fe(Cu)$ peritectic phase with hexagonal crystal structure, also was observed in the form of platelets or an indefinite-shaped. According to Taylor et al. [5], at lower iron concentrations (< 0.1% Fe) there are more Chinese-script π phase than β-Al_5FeSi, which sometimes grows from and/or surrounding the β platelets. However, this was not observed in the present work. Also, the Mg_2Si phase was not observed and possibly the entire Mg was dissolved in the λ and π phases. In according to Samuel [6] the presence of Mg segregates both Fe and Cu, forming intermetallic compounds in areas away from the silicon eutectic. On the other hand, the Al_2Cu phase with tetragonal crystal structure precipitates in two distinct morphologies: Al-Al_2Cu eutectic and in the form of blocky phase with high copper concentration (~38-40 wt%). It is observed that a dramatic increase in the porosity occurs when the Cu level increases beyond 0.2%

[1]. During planar or dendritic solidification, the Al_2Cu phase grows cooperatively with the α-Al with the same morphology as in binary alloys independently of the presence of silicon [7].

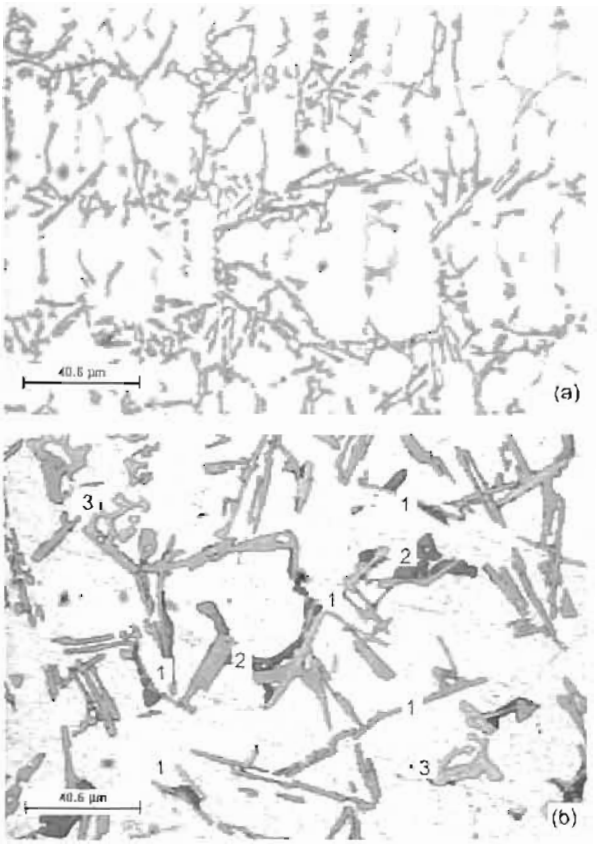

Figure 3. Optical micrograph of as-cast typical microstructure of the alloy: (a) 2 and (b) 3. (1) β-Al_5FeSi, (2) Al_2Cu and (3) $Al_{15}(MnFe)_3Si_2$.

The β-Al_5FeSi with monoclinic crystal structure precipitates in the interdendritic and intergranular regions as platelets (appearing as needles in metallographic sections). This phase was scarcely observed in the alloy 2 (figure 4a), due to the low iron contents. While in the alloy 3 (figures 4b and 6) it was observed a significant increase in its content. Taylor et al [5] suggests that the length and the average number of these iron-containing intermetallic particles, increase linearly with the iron content. Samuel [7] observed in its experiments, that at the lower cooling rates and large secondary dendritic spacings, the length of the β-Al_5FeSi platelets is larger. At lower cooling rate, time for diffusion in front of the solid/liquid interface is larger implying in a more intensive flux of atoms and thus, larger quantity of atoms of iron may be rejected, contributing to the formation of large β platelets. Other works indicate, also, that iron exhibits a strong threefold influence on porosity and shrinkage-defect formation [5, 8]. The same authors suggest that the β-Al_5FeSi platelets restrict feeding. Since the platelets form in the channels during solidification, they cause physical restrictions to the movement of compensatory feed liquid. This phase is considered as active pore nucleation site and also physically constrainer the pores growth [8].

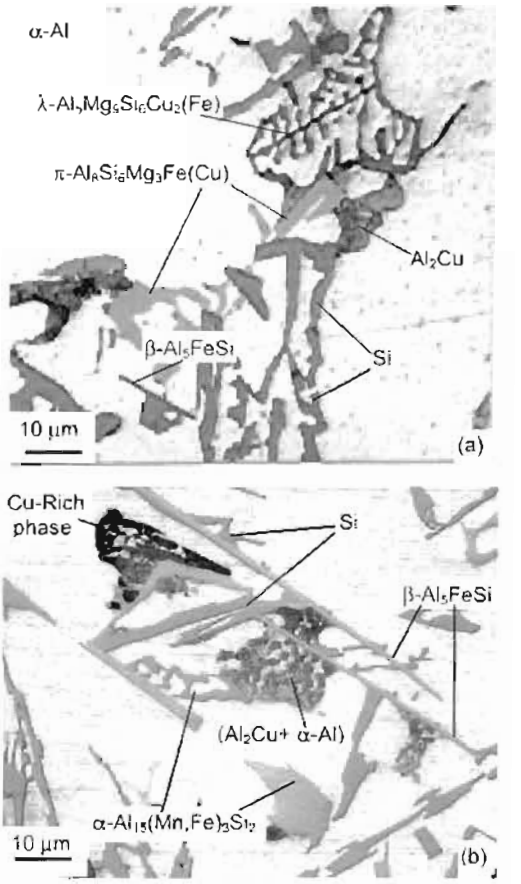

Figure 4 Optical micrographs showing microstructures of the interdendritic region of the alloy: (a) 2 and (b) 3.

In the alloy 3 (figures 4 and 6), the platelets appeared to be the main nucleation sites for the eutectic silicon, eutectic Al_2Cu and Cu-rich phase. Nucleation of silicon (both acicular and polygonal) and Al_2Cu may occur on large β-Al_5FeSi platelets, between Al-(β-Al_5FeSi) binary eutectic complex and on the smaller β-Al_5FeSi platelets (formed as a component of Al-Si-Al_5FeSi complex ternary eutectic). The silicon was frequently observed to grow from multiple locations along single β-platelet and even, on occasion, to engulf completely smaller β-platelets.

Another common intermetallic in the Al-Si-Cu system is the α-$Al_{15}(Mn,Fe)_3Si_2$ phase, also known as α-Al_8Fe_2Si phase with cubic crystal structure. This phase has a compact morphology, which does not initiate cracks in the cast material to the same extent as the β-Al_5FeSi, despite its elevated hardness [4]. The α-$Al_{15}(Mn,Fe)_3Si_2$ phase shows, in contrast to the β-Al_5FeSi, some variations in composition and quite different morphologies depending on the cooling conditions. At low cooling rates

the α-$Al_{15}(Mn,Fe)_3Si_2$ phase is formed as primary crystals. However, when the cooling rate increases, those crystals suffer a morphology transition, to a typical "Chinese script" form or to a fine eutectic structure, as observed in the figure 5c. This phase appears in the interdendritic and intergranular regions (figures 3b, 4b and 5). Close to the dendritic region (figure 3b) the α-$Al_{15}(MnFe)_3Si_2$ phase is partly supresed in its growth. However, in areas away of the interdendritic region, inside α-Al dendrites, the α-$Al_{15}(MnFe)_3Si_2$ and α-Al phases solidify simultaneously, as shown in the table 2.

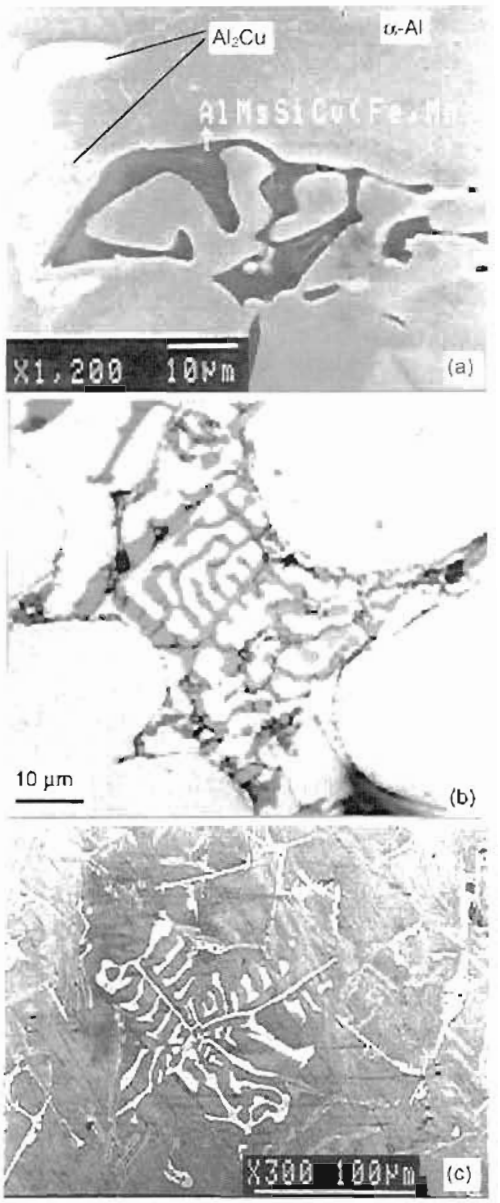

Figure 5. Chinese script morphologies, in the alloy 2 (a) λ-$Al_5Mg_9Si_6Cu_2(Fe)$, (b) π-$Al_8Si_6Mg_3Fe(Cu)$, and in the alloy 3 (c) α-$Al_{15}(MnFe)_3Si_2$.

Due to the detrimental effect of the β-Al_5FeSi phase, their formation is avoided through additions of alloying elements, mainly of Mn [4, 5] and Be [9]. They alter the composition and morphology of β-plates into Chinesse script and polygons, found mostly inside α-Al dendrites. Analysis of EDS indicates that the chemical composition of intermetallic phases varies in a certain interval, as shown in the table 3.

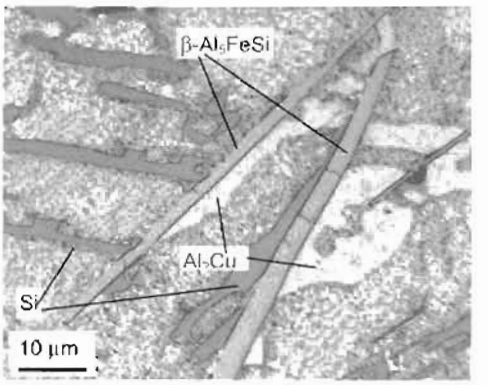

Figure 6. Microstructure: showing eutectic silicon and Al_2Cu nucleating on β-Al_5FeSi platelets, (alloy 3).

Table 3. Compositions of experimentally observed intermetallic phases (at. %).

Phase	Al	Mg	Si	Fe	Cu	Mn	Refer.
β-Al_5FeSi	64.0		19.4	16.6			[10]
	67.7		16.5	15.8			[11]
	73.8		11.4	14.8			This work
π-$Al_8Si_6Mg_3Fe$	51.4	15.2	28.3	5.1			[10]
	51.7	15.0	27.4	5.9			[11]
	47.3	18.8	28.5	5.4			This work
α-$Al_{15}(MnFe)_3Si_2$	68.7		11.8	12.2	0.8	6.1	[4]
	64.0		10.1	19.8	3.7	2.0	[4]
	63.9		8.3	19.6	2.5	5.7	This work

The figure 5b shows an example of fragmentation of the π-$Al_8Si_6Mg_3Fe(Cu)$ phase in small particles, possibly, because it was trapped and pressed by the dendritic arms. Also, it is observed in the figure 6 that the β-Al_5FeSi phase is completely brittle, since its particles break during polishing in slurry of alumina. It suggests that the intermetallic phases may act as stress raisers and crack initiation sites that reduce the strength and ductility of the Al-Si-Cu alloys, due to the lack of active slip systems in the intermetallic compounds.

Conclusions

The alloys studied in the current work possess complex morphologies and as-cast microstructures. Depending on the composition of the alloys, complex binary, ternary and quaternary eutectic structures are

formed. High iron concentrations form intermetallic phases that are undesirable in the commercial aluminum alloys. The β-Al_5FeSi phase is the most harmful among the intermetallic phases in the Al-Si-Cu system. Besides being highly brittle, it acts as nucleation site for silicon and Al_2Cu.

Acknowledgment

Authors acknowledge the FAPESP for the financial support.

References

1. Chang, J., Moon, I., Choi, C., *J. Mater. Sci*, v.33, p.5015, (1998).

2. Anantha Narayanam, L., Samuel, F. H., Gruzleski, J. E., *Metall. Mater. Trans.* v.26A, p.2161, (1995).

3. Mondolfo L. F., Aluminum alloys: structure and properties, 1st ed., London, Butterworths, (1976).

4. Bäckerud, L., Chai, G., Tamminen, J., Solidification Characteristics of Aluminum Alloys – Foundry Alloys, Ed. AFS/Skanaluminium, Sweden, v.2, (1990).

5. Taylor, J. A., Schaffer, G. B., StJohn, D. H., *Metall. Mater. Trans. A*, v.30A, p.1643, (1999).

6. F. H. Samuel, *J. Mat. Sci.*, v.33, p.2283, (1998).

7. F. W. Schnake, G. A. Varschavsky, *Metallography*, v.11, p.459, (1978).

8. Roy, N., Samuel, A. M., Samuel, F. H., *Metall. Mater. Trans.* A, v.27A, p.415, (1996).

9. Murali, S., Raman, K. S., Murthy, K. S. S., *Mat. Sci. Eng.*, v.A190, p.165, (1995).

10. Closet, B., Gruzleski, J. E., *Metall. Trans.* v.13A, p.945, (1982).

11. Liu, Y. L., Kang, S. B., Kim, H. W., *Materials Letter*, v.41, p.267, (1999).